



Research paper

Implementation of state-averaged MCSCF method to RISM- and 3D-RISM-SCF schemes

Daisuke Okamoto, Yoshihiro Watanabe, Norio Yoshida*, Haruyuki Nakano*

Department of Chemistry, Graduate School of Science, Kyushu University, Fukuoka 819-0395, Japan

HIGHLIGHTS

- State-averaged MCSCF in RISM-SCF was formulated as a quasi-variational problem.
- Basis equations were derived by variational conditions of two Helmholtz energies.
- The method gives multiple states and a solvation structure simultaneously.
- It was applied to potential energy and electronic transition of molecules in water.

ARTICLE INFO

Keywords:

State-averaged MCSCF
Integral equation theory of liquids
RISM-SCF
3D-RISM-SCF

ABSTRACT

The state-averaged multiconfiguration self-consistent field (MCSCF) method was implemented to the reference interaction site model and three-dimensional reference interaction site model (RISM and 3D-RISM) SCF schemes, where the electronic structures of multiple states and solvation structure are determined simultaneously by the state-averaged MCSCF method and state-specific RISM-SCF/3D-RISM-SCF scheme, respectively, in a single calculation. The method was applied to the potential energy curves of the low-lying states of NaCl in aqueous solution and solvation shifts of the excitation energy of formaldehyde and *p*-nitroaniline. The results showed good agreement with those of the state-specific MCSCF and/or experiments.

1. Introduction

The multiconfiguration self-consistent field (MCSCF) method is one of the basic methods in modern electronic structure theory for molecules [1]. Because of the multiconfigurational nature of the wavefunctions that the method inherently employs, the MCSCF method can treat multiconfigurational electronic states for which the Hartree–Fock method or density functional theory (DFT) is not applicable, that is, systems in radical bond-breaking, low-spin states of transition metal systems, or excited electronic states. For this reason, versions of the MCSCF method using various variational space definitions, for example, complete [2,3], quasi-complete [4], restricted [5], occupation-restricted multiple [6], and generalized [7] active spaces (CAS, QCAS, RAS, ORMAS, and GAS, respectively) have been developed. Furthermore, multireference methods based on perturbation theory, configuration-interaction (CI), and coupled-cluster approaches to compensate for the semiquantitative accuracy of the MCSCF method have been developed and are now included in standard quantum chemistry program packages. In addition to the state-specific (or pure-state) MCSCF

(SS-MCSCF) method that determines the wavefunction of a single state, the state-averaged MCSCF (SA-MCSCF) method is commonly used. Because the SA-MCSCF method minimizes an averaged energy of multiple states, it is not a pure variational approach. However, it has several advantages such as being able to obtain multiple states simultaneously, being able to compute interstate matrix elements, and being stable even if the calculation includes excited states. Therefore, the SA-MCSCF method is a very effective approach, especially for excited states.

In the 1990s, Ten-no, Hirata, and Kato presented a method that combines ab initio electronic structure theory of molecules and integral equation theory of molecular liquids, which is called the reference interaction site model self-consistent field (RISM-SCF) method [8,9]. They derived coupled equations of Hartree–Fock and RISM equations. These coupled equations are solved self-consistently and give the electronic wavefunction of the solute molecule and the solvent distribution simultaneously. Since this pioneering work, the combination of the two theories has been extended both in the integral equation and electronic structure theories. Kovalenko and Hirata developed a

* Corresponding authors.

E-mail addresses: noriwo@chem.kyushu-univ.jp (N. Yoshida), nakano@chem.kyushu-univ.jp (H. Nakano).<https://doi.org/10.1016/j.cplett.2019.05.051>

Received 3 April 2019; Received in revised form 25 May 2019; Accepted 29 May 2019

Available online 29 May 2019

0009-2614/ © 2019 Elsevier B.V. All rights reserved.

combined method of the Kohn–Sham DFT and the 3D-RISM (KS-DFT/3D-RISM) [10], which was followed by the works of Gusarov, Ziegler, and Kovalenko [11], and Casanova, Gusarov, Kovalenko, and Ziegler [12] in 2000s. This method was further extended by Sato, Kovalenko, and Hirata to the use of the molecular orbital (MO) method instead of KS-DFT [13]. Yoshida and Kato proposed a combination of ab initio electronic structure theory and the molecular Ornstein–Zernike (MOZ) integral equation theory, referred to as the MOZ-SCF method [14]. At present, RISM-SCF methods for the MCSCF method [15], the second-order Møller–Plesset perturbation theory [16], the coupled-cluster singles and doubles method [17], and the density matrix renormalization group SCF method [18] are also implemented. These methods have been applied to various problems [19].

The combination of the MCSCF method and integral equation theory was achieved by Sato, Hirata, and Kato [15]. This method is particularly attractive from the above-mentioned advantages of the MCSCF method, such as the simultaneous solution of multiple states and description of multiconfigurational states. These advantages have been successfully carried over into calculations of molecules in solution thanks to their method. However, their formulation of the MCSCF-based RISM-SCF method was limited to a state-specific MCSCF treatment. Thus, the merits of the MCSCF method have not been utilized fully. It should be noted that although the use of the state-averaged MCSCF method has also been reported in a few literatures, they were done under the assumption that the excess chemical potentials of the averaged states were all equal [20,21]. In this Letter, we implement the state-averaged MCSCF method to the RISM-SCF scheme, where multiple states are solved by the MCSCF method in electronic structure theory while a specific state is handled in the integral equation theory. The method is described in Section 2 and is applied to several systems (potential energy curves (PECs) of NaCl in aqueous solution and solvation shifts of excitation energies in formaldehyde and *p*-nitroaniline (PNA)) in Section 3, and conclusions are derived in Section 4.

Note that in the present Letter, two kinds of self-consistent *field* are used by convention: that is, the electric *field* caused by electrons in occupied MOs in MCSCF and that caused by the solvent charge distribution in RISM-SCF. The former and latter electric fields are determined self-consistently inside the MCSCF process and between the MCSCF and RISM processes, respectively.

2. Method

Sato et al. formulated RISM-SCF based on MCSCF as a variational problem of the Helmholtz energy [15]. They derived basic equations by minimizing the Helmholtz energy for a specific state X :

$$A_X = E_X + \Delta\mu_X, \quad (1)$$

for both the wavefunction variation and solvent distribution variation, where X is the state for which solvent distribution is to be determined, and E_X and $\Delta\mu_X$ are the energy of the solute in the specific state X and the excess chemical potential, respectively. Because the state-averaged MCSCF is not a variational approach to a single energy, it is necessary to introduce one more functional to be minimized, namely, a state-averaged Helmholtz energy:

$$\begin{aligned} A^{\text{ave}} &= \sum_I^{\text{state}} w_I (E_I + \Delta\mu_I^{(X)}) \\ &= E^{\text{ave}} + \Delta\mu^{(X)\text{ave}}, \end{aligned} \quad (2)$$

where w_I are averaging weights. The variational conditions for RISM-SCF based on state-averaged MCSCF are separated into two, that is, the condition for the state-averaged Helmholtz energy, Eq. (2), for the wavefunction variations, and the condition for the Helmholtz energy for the specific state X , Eq. (1), for solvent distribution variations. In Eq. (2), the solute energy E_I and averaged solute energy E^{ave} are defined as:

$$\begin{aligned} E_I &= \langle \Psi_I | \hat{H} | \Psi_I \rangle \\ &= \sum_{ij}^{\text{MO}} \langle \phi_i | \hat{h} | \phi_j \rangle \gamma_{ij}^I + \frac{1}{2} \sum_{ijkl}^{\text{MO}} \langle \phi_i \phi_k | r_{12}^{-1} | \phi_j \phi_l \rangle \Gamma_{ij,kl}^I, \end{aligned} \quad (3)$$

and

$$\begin{aligned} E^{\text{ave}} &= \sum_I^{\text{state}} w_I \langle \Psi_I | \hat{H} | \Psi_I \rangle \\ &= \sum_{ij}^{\text{MO}} \langle \phi_i | \hat{h} | \phi_j \rangle \gamma_{ij}^{\text{ave}} + \frac{1}{2} \sum_{ijkl}^{\text{MO}} \langle \phi_i \phi_k | r_{12}^{-1} | \phi_j \phi_l \rangle \Gamma_{ij,kl}^{\text{ave}}, \end{aligned} \quad (4)$$

where \hat{H} and \hat{h} are the total and one-electron Hamiltonians of the isolated solute molecule, respectively, and ϕ_i and Ψ_I are the one-electron wavefunctions (i.e., MOs) and the many-electron wavefunctions, respectively. The symbols γ_{ij}^I and $\Gamma_{ij,kl}^I$ are one- and two-electron density matrices for state I , respectively, and γ_{ij}^{ave} and $\Gamma_{ij,kl}^{\text{ave}}$ are their state-averaged values. The expression for the excess chemical potential is dependent on basic equations used in the integral equation theory. Here, take the RISM equation and the hypernetted chain (HNC) equation, for example, following Ref. [15], the expression becomes:

$$\begin{aligned} \Delta\mu_I^{(X)} &= -k_B T \rho \sum_{\alpha}^U \sum_s^V \int d\mathbf{r} \{ \exp[-u_{\alpha s}^I(r)/k_B T + h_{\alpha s}^X(r) - c_{\alpha s}^X(r)] \\ &\quad - 1 - h_{\alpha s}^X(r) + c_{\alpha s}^X(r) - h_{\alpha s}^X(r)[h_{\alpha s}^X(r)/2 - c_{\alpha s}^X(r)] \\ &\quad - (k_B T/8\pi^3) \int d\mathbf{k} \left\{ - \sum_{\alpha}^U \sum_s^V \hat{c}_{\alpha s}^X(k) \hat{\rho}_{\alpha s}^X(k) \right. \\ &\quad \left. + (1/2) \sum_{\alpha\gamma}^U \sum_{st}^V \hat{c}_{\alpha s}^X(k) \hat{c}_{\gamma t}^X(k) \hat{\omega}_{\alpha\gamma}^X(k) \hat{\chi}_{st}^X(k) \right\} \end{aligned} \quad (5)$$

where $h_{\alpha s}^X(r)$ and $c_{\alpha s}^X(r)$ are the total and direct correlation functions for state X ($\hat{h}_{\alpha s}^X(k)$ and $\hat{c}_{\alpha s}^X(k)$ are their Fourier transformed functions), respectively, and U and V are solute and solvent sites, respectively. $\hat{\omega}_{\alpha\gamma}^X(k)$ is the intramolecular correlation function of the solute, and $\hat{\chi}_{st}^X(k)$ is the density correlation function of the solvent, both of which are in wavenumber expression. Eq. (5) includes the solute–solvent interaction dependent on states I to be averaged:

$$u_{\alpha s}^I(r) = \frac{q_{\alpha}^I q_s}{r} + u_{\alpha s}^*(r), \quad (6)$$

where $u_{\alpha s}^*(r)$ is the short-range interaction, typically given by the Lennard–Jones (LJ) potential and q_s are solvent charges. The solute charge q_{α}^I is given through the one-electron density matrix γ_{ij}^I for state I generated from the MCSCF process:

$$q_{\alpha}^I = - \sum_{ij}^{\text{MO}} \langle \phi_i | \hat{b}_{\alpha} | \phi_j \rangle \gamma_{ij}^I, \quad (7)$$

where the \hat{b}_{α} are population operators [22]. Note that the expression Eq. (5) is dependent on both the specific state X for which the solvent distribution is determined and states I which are averaged in the MCSCF process, and $\Delta\mu_X$ in Eq. (1) is a special case of $\Delta\mu_I^{(X)}$ when $I = X$.

In the MCSCF method, the wavefunction variations can be split into a one-electron wavefunction variation part $\delta\phi_i$ and many-electron wavefunction variation part $\delta\Psi_I$, which corresponds to MO/CI coefficient changes for fixed CI/MO coefficients. Taking variations of Eq. (2) for ϕ_i and Ψ_I :

$$\frac{\delta A^{\text{ave}}}{\delta\phi_i} = \frac{\delta A^{\text{ave}}}{\delta\Psi_I} = 0, \quad (8)$$

under binding conditions:

$$\langle \phi_i | \phi_j \rangle = \delta_{ij}, \quad \langle \Psi_I | \Psi_J \rangle = \delta_{IJ}, \quad (9)$$

we obtain the following MCSCF equations. One is the MO equation:

$$x_{pq} = x_{qp}, \quad (10)$$

where x_{pq} are the Lagrangians in the MCSCF method:

$$x_{pq} = \sum_i^{\text{MO}} \left\langle \phi_p \left| \hat{h} + \sum_{\alpha} V_{\alpha}^X \hat{b}_{\alpha} \right| \phi_i \right\rangle \gamma_{qi}^{\text{ave}} + \sum_{ijk}^{\text{MO}} \langle \phi_p \phi_i | r_{12}^{-1} | \phi_k \phi_j \rangle \Gamma_{qk,ij}^{\text{ave}}, \quad (11)$$

and the other is the CI equation:

$$\left(\hat{H} + \sum_{\alpha} V_{\alpha}^X \hat{b}_{\alpha} \right) |\Psi_I\rangle = E_I |\Psi_I\rangle, \quad (12)$$

to determine the CI coefficients in $|\Psi_I\rangle = \sum_A C_A^I |\Phi_A\rangle$ ($|\Phi_A\rangle$: Slater determinants). Here, V_{α}^X is the electrostatic potential (ESP) on solute site α :

$$V_{\alpha}^X = \rho \sum_s^V q_s \int \frac{g_{\alpha s}^X(r)}{r} dr, \quad (13)$$

coming from solvent site charges q_s and radial distribution function $g_{\alpha s}^X(r) = h_{\alpha s}^X(r) + 1$, and \hat{b}_{α} is the many-electron population operator:

$$\hat{b}_{\alpha} = \sum_i^{\text{electron}} \hat{b}_{\alpha}(i). \quad (14)$$

On the other hand, taking variations of Eq. (1) for $h_{\alpha s}^X(r)$ and $c_{\alpha s}^X(r)$:

$$\frac{\delta A^X}{\delta h_{\alpha s}^X} = \frac{\delta A^X}{\delta c_{\alpha s}^X} = 0, \quad (15)$$

we obtain the RISM and HNC closure equations:

$$\rho h_{\alpha s}^X(r) = \sum_{\gamma}^U \sum_t^V \omega_{\alpha\gamma}^X * c_{\gamma t}^X * \chi_{ts}^X(r), \quad (16)$$

and

$$c_{\alpha s}^X(r) = \exp[-u_{\alpha s}^X(r)/k_B T + h_{\alpha s}^X(r) - c_{\alpha s}^X(r)] - [h_{\alpha s}^X(r) - c_{\alpha s}^X(r)] - 1, \quad (17)$$

where $\omega_{\alpha\gamma}^X(r)$ and $\chi_{ts}^X(r)$ are the intramolecular correlation function of the solute and the density correlation function of the solvent in coordinate expression, respectively, and the asterisk * means the convolution integral. Their definitions are the same as those used in ordinary RISM theory and given elsewhere.[8]

The two couples of Eqs. (10) and (12) and Eqs. (16) and (17) are solved iteratively. Fig. 1 shows the RISM-SCF scheme, that is, the procedure for solving the equations. During the MCSCF iteration, the state-averaged one- and two-electron densities are used, and after the convergence of the iteration, the state-specific one-electron density is calculated. This state-specific density is passed to the RISM program. In the RISM solution process, the state-specific calculations are performed to give the state-specific solvent distribution. The electrostatic potential due to the solvent distribution is returned to the MCSCF program. These

processes are repeated until the convergence of both the wavefunctions of multiple states and the solvent distribution.

The applications of the above-mentioned procedure to other integral equation theories and closure relations are straightforward. The present method is implemented for RISM, 3D-RISM, and MOZ integral equation theories (as well as other closures such as the Kovalenko–Hirata closures) in the modified version [23] of GAMESS [24]. Our integral equation theory program allows not only state-specific calculations, but also state-averaging calculations (with a different weight from that in the MCSCF part), thereby being also applicable to degenerate electronic states.

3. Computational details

To demonstrate the present method, we applied it to the PECs of NaCl in aqueous solution and solvation shifts of the excitation energies of the $n-\pi^*$ transition of formaldehyde and the $\pi-\pi^*$ transition of PNA. The state-averaged MCSCF calculations with 1D- and/or 3D-RISM were performed for NaCl (1D), formaldehyde (1D and 3D), and PNA (1D and 3D) in aqueous solution. In the NaCl calculations, the active space used was CAS(6,7) constructed from six electrons and seven MOs. Four states, $1^1\Sigma$, $2^1\Sigma$, $1^1\Pi$, and $1^1\Pi'$ were averaged. In the formaldehyde calculations, the active space used was multireference configurations plus singles and doubles (MRSD)-type constructed from 12 electrons, 18 MOs, and 2 parent configurations. The parent configurations were the closed-shell and HOMO–LUMO ($n-\pi^*$) excited configurations, which constitute the MRSD active space with singles and doubles from the parent configurations. Two states, the ground and $n-\pi^*$ excited states, were averaged. In the PNA calculations, the active space was MRSD-type constructed from 28 electrons, 26 MOs, and 2 parent configurations. The parent configurations were the closed-shell and HOMO–LUMO ($\pi-\pi^*$) excited configurations, which constitute the MRSD active space with singles and doubles from the parent configurations. Two states, the ground and $\pi-\pi^*$ excited states, were averaged. In all the calculations, the correlation-consistent polarized valence triple zeta (cc-pVTZ) basis set [25–27] was used. The molecular structure of formaldehyde was optimized using the RISM-SCF/DFT method and the molecular structure of PNA was optimized using the KS-DFT with the polarizable continuum model (PCM) [28], where the PBE0 hybrid functional [29,30] was used in the DFT calculation. In addition, for comparison, the state-specific MCSCF calculations and MCSCF reference perturbation calculations (the perturbation theory with general MCSCF reference wavefunctions, GMCPT [31,32]) were also carried out.

The parameters used in the 1D- and 3D-RISM-SCF method were as follows. The temperature and density of solvent water were 298.15 K and 0.0333 molecules per \AA^3 , respectively. Effective point charges were used to describe the solute–solvent interaction potential in the RISM-SCF calculations. The effective point charges on the solute molecule

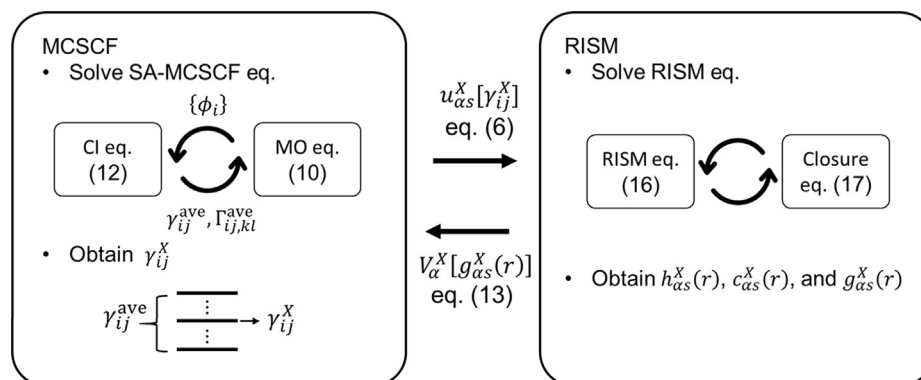


Fig. 1. RISM-SCF scheme using SA-MCSCF method.

were determined to reproduce the electrostatic potential around the solute molecule using a least-square fitting. The pairs of LJ parameters (σ in Å, ϵ in kcal/mol) were (3.328, 0.00277) for Na and (4.401, 0.1) for Cl in the NaCl calculations [33], (3.55, 0.07) for C, (0.4, 0.046) for H, and (2.96, 0.17) for O in the formaldehyde calculations [34,35], and (3.55, 0.07) for C, (2.42, 0.03) for H, (3.25, 0.12) for N of the nitro group, (3.25, 0.17) for N of the amino group, and (2.96, 0.17) for O in the PNA calculations [34,35]. The extended simple point charge model (SPC/E) parameter set for the geometrical and potential parameters for the solvent water was used with modified H parameters ($\sigma = 1.0$ Å and $\epsilon = 0.056$ kcal/mol) [36]. There were 4096 grid points with a spacing of 0.05 Å in the 1D-RISM calculations, and in the 3D-RISM calculations, there were $256 \times 256 \times 256$ with a spacing of 0.10 Å for formaldehyde and $128 \times 128 \times 128$ with a spacing of 0.25 Å for PNA. In all cases, the target state of the 1D- and 3D-RISM calculations was the ground state.

In the following sections, we use 1D-RISM-SCF instead of RISM-SCF to distinguish it clearly from 3D-RISM-SCF. In addition, for simplicity, we use a notation of SA-MCSCF/1D-RISM, which indicates a state-specific 1D-RISM-SCF calculation using the state-averaged MCSCF method. We further use a notation of SA-MCSCF//SS-MCSCF/1D-RISM, which means a state-averaged MCSCF calculation using the ESP generated by the SS-MCSCF/1D-RISM calculation.

4. Applications

The NaCl molecule is connected with an ionic bond in a vacuum. This molecule has $1^1\Sigma$ and $2^1\Sigma$ PECs that show avoided crossing, and dissociative $1^1\Pi$ and $1^1\Pi'$ PECs, which are widely known and seen elsewhere [37]. In aqueous solution, the ionic electronic state is the most stable and its PEC is dissociative. Fig. 2 compares the PECs of the ground state in aqueous solution calculated by the present method (SA-MCSCF/1D-RISM) and SS-MCSCF/1D-RISM, and Fig. 3 shows the difference between the PECs by the two methods. The potential energies themselves are considerably different, as is often the case in the calculations of systems including bulk such as a solvent. More important than the agreement of PECs themselves is the agreement of the shape of the PECs, and its difference is estimated from Fig. 3 to be about 0.14 eV at around 3 Å. Fig. 4 compares the PECs of the four states calculated by the present method (SA-MCSCF/1D-RISM) and SA-MCSCF//SS-MCSCF/1D-RISM, and Fig. 5 shows the difference between the PECs by the two

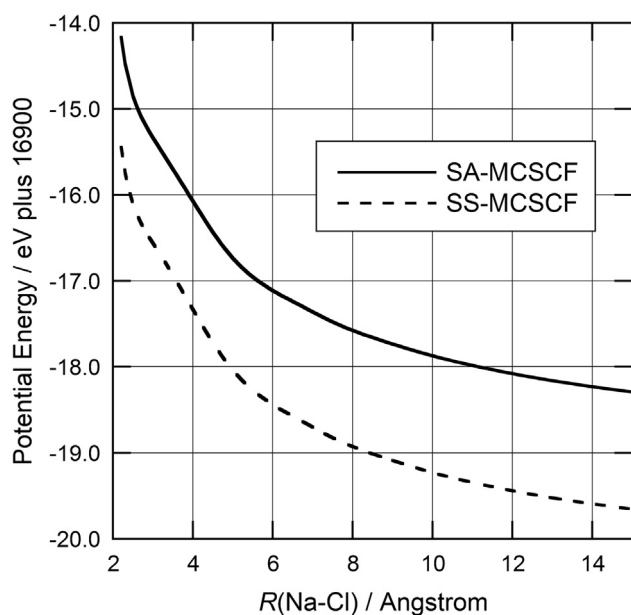


Fig. 2. The PECs of the ground ($1^1\Sigma$) state of NaCl calculated using SA-MCSCF/1D-RISM and SS-MCSCF/1D-RISM.

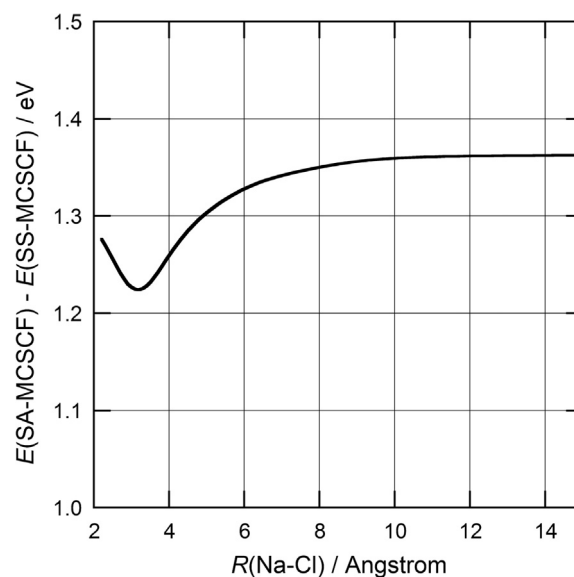


Fig. 3. Difference between the PECs of SA-MCSCF/1D-RISM and SS-MCSCF/1D-RISM in Fig. 2.

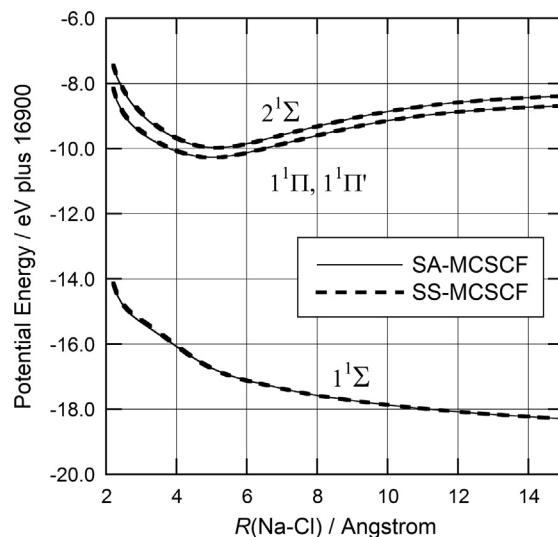


Fig. 4. The PECs of the $1^1\Sigma$, $2^1\Sigma$, $1^1\Pi$, and $1^1\Pi'$ states of NaCl calculated using SA-MCSCF/1D-RISM and SA-MCSCF//SS-MCSCF/1D-RISM.

methods. The PECs by the two methods are close to each other. The maximum difference was 0.205 eV at around 3 Å. These results indicate that the present method provides close PECs to those of SS-MCSCF/1D-RISM.

Formaldehyde has the $n-\pi^*$ lowest singlet excited state transition. Table 1 shows the excitation energy and its solvation shift of the $n-\pi^*$ transition of formaldehyde calculated using the 1D- and 3D-RISM-SCF methods. The excitation energy by SA-MCSCF in the gas phase was 4.34 eV. The present method (SA-MCSCF/1D- and 3D-RISM) gave 4.62 and 4.58 eV in the 1D- and 3D-RISM-SCF cases, respectively; hence the solvation shift was 0.28 and 0.24 eV, respectively. The experimental excitation energy was 4.07 and 4.28 eV in the gas phase and aqueous solution and therefore the solvation shift was 0.21 eV [38,39]. The present method gave a qualitatively correct and semiquantitative shift, although the method slightly overestimated the shift. These results are quite reasonable considering the accuracy of the MCSCF method. The SA-MCSCF method using the ESP generated by ground-state-specific MCSCF (SA-MCSCF//SS-MCSCF/1D- and 3D-RISM) underestimated the solvation shift. The shifts for the ESP by 1D- and 3D-RISM-SCF were

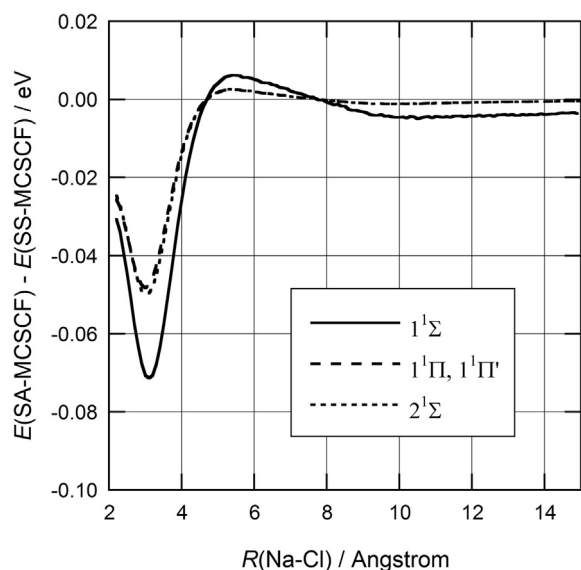


Fig. 5. Differences between the PECs of the $1^1\Sigma$, $2^1\Sigma$, $1^1\Pi$, and $1^1\Pi'$ states of NaCl calculated using SA-MCSCF/1D-RISM and SA-MCSCF//SS-MCSCF/1D-RISM in Fig. 4.

both 0.10 eV, about half the experimental value. The GMCPT improved the shift as well as the excitation energy. The shifts by GMCPT using the ESP by the present method (GMCPT//SA-MCSCF/1D- and 3D-RISM) were 0.21 and 0.19 eV, respectively. Those using the ESP by SS-MCSCF/1D- and 3D-RISM-SCF were 0.14 and 0.17 eV, respectively. The results of the present method were somewhat better even after inclusion of more electronic correlation by GMCPT.

Fig. 6(a) and (b) compare two sets of radial distribution functions (RDFs) of formaldehyde: Fig. 6(a) and (b) show the RDFs by SA-MCSCF/1D-RISM and SS-MCSCF/1D-RISM, respectively. The figures include the RDF of solvents H from the solute O (RDF(O–H_w)) and that of solvents O from a solute H (RDF(H–O_w)). The two sets of RDFs are close to each other, though the first peaks of RDF(O–H_w) and RDF(H–O_w) in Fig. 6(a) are somewhat higher and narrower than those in Fig. 6(b). The positions of the first and second peaks of RDF(O–H_w) in Fig. 6(a) are 1.7 and 3.8 Å, respectively, and those in Fig. 6(b) are 1.8 and 3.8 Å, respectively. Similarly, the positions of the first and second peaks of RDF(H–O_w) in Fig. 6(a) are 1.7 and 4.0 Å, respectively, and those in Fig. 6(b) are 1.8 and 4.0 Å, respectively.

The solvation shift values in Table 1 and the difference in peak

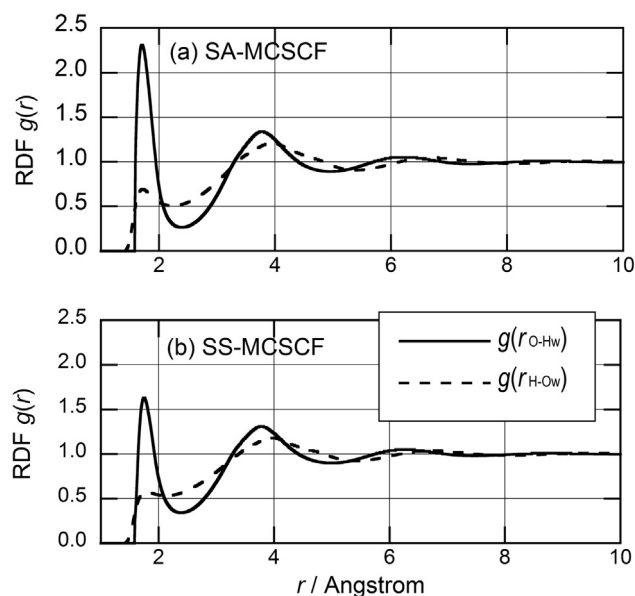


Fig. 6. The RDFs of H of water (H_w) from the solute O and RDFs of O of water (O_w) from a solute H in formaldehyde solution calculated using (a) SA-MCSCF/1D-RISM and (b) SS-MCSCF/1D-RISM.

height in Fig. 6 indicate that the SA-MCSCF shows slightly larger solute–solvent interaction than that of the SS-MCSCF. The reason is the polarization of formaldehyde is overestimated by the SA-MCSCF compared with the SS-MCSCF. The dipole moments of formaldehyde in the gas phase calculated by SA-MCSCF and SS-MCSCF were 2.7 and 2.1 Debye, respectively, and those in aqueous solution calculated by SA-MCSCF/1D-RISM and SS-MCSCF/1D-RISM were 4.2 and 3.3 Debye, respectively. Similar trend was also observed in the 3D-RISM case.

PNA has a charge-transfer-type lowest singlet excited state. Thus, for a polar solvent, it shows a redshift of the corresponding absorption band. Table 2 shows the excitation energy and its solvation shift of the lowest singlet π – π^* charge-transfer excitation of PNA calculated by 1D- and 3D-RISM-SCF methods. The excitation energy by SA-MCSCF in the gas phase was 5.09 eV. The present method (SA-MCSCF/1D- and 3D-RISM) gave 4.89 and 4.73 eV in the 1D- and 3D-RISM-SCF cases; that is, the solvation shift was –0.80 and –0.96 eV, respectively. In experiments, a shift of –0.98 eV (4.24 eV in the gas phase [40] and 3.26 eV in aqueous solution [41,42]) was observed. It is known that the MCSCF method significantly overestimates the excitation energies of charge-

Table 1

Vertical excitation energy and solvation shift for the n – π^* singlet excited state of formaldehyde (in eV).

Method ^a	SA-MCSCF/RISM	-	SS-MCSCF/RISM	-	Exp.
	SA-MCSCF ^b	GMCPT ^c	SA-MCSCF ^d	GMCPT ^e	
<i>1D-RISM</i>					
Excitation energy ^f	4.62 (4.34)	4.22 (4.01)	4.45 (4.34)	4.15 (4.01)	4.28 ^g (4.07 ^h)
Solvation shift	0.28	0.21	0.10	0.14	0.21
<i>3D-RISM</i>					
Excitation energy	4.58	4.20	4.45	4.18	4.28 ^g
Solvation shift	0.24	0.19	0.10	0.17	0.21

^a The first and second lines denote the RISM-SCF method that determined the solvation distribution and the electronic structure method that computed the excitation energy.

^b Present method (SA-MCSCF/1D- or 3D-RISM).

^c GMCPT//SA-MCSCF/1D- or 3D-RISM.

^d SA-MCSCF//SS-MCSCF/1D- or 3D-RISM.

^e GMCPT//SS-MCSCF/1D- or 3D-RISM.

^f The numbers in parentheses are excitation energies in the gas phase.

^g Reference [39].

^h Reference [38].

Table 2
Vertical excitation energy and solvation shift for the π - π^* singlet excited state of PNA (in eV).

Method ^a	SA-MCSCF/RISM	-	SS-MCSCF/RISM	-	Exp.
	SA-MCSCF	GMCPT	SA-MCSCF	GMCPT	
<i>1D-RISM</i>					
Excitation energy ^b	4.89 (5.69)	4.15 (4.39)	4.82 (5.69)	4.03 (4.39)	3.26 ^c (4.24 ^d)
Solvation shift	-0.80	-0.24	-0.87	-0.36	-0.98
<i>3D-RISM</i>					
Excitation energy	4.73	3.94	4.64	4.03	3.26 ^c
Solvation shift	-0.96	-0.45	-1.04	-0.36	-0.98

^a The explanations of the methods are the same as in Table 1.

^b The numbers in parentheses are excitation energies in the gas phase.

^c References [41] and [42].

^d Reference [40].

transfer states. The calculated excitation energy is considerably larger than the experimental value. However, regarding the shift, the present method gave reasonable values, especially in the 3D-RISM-SCF case. These features can also be seen in the results of the SA-MCSCF using the ESP generated by SS-MCSCF/1D- and 3D-RISM (SA-MCSCF//SS-MCSCF/1D- and 3D-RISM). The shifts were -0.87 eV in the 1D-RISM-SCF case (5.69 → 4.82 eV from gas to aqueous phase) and -1.04 eV in the 3D-RISM-SCF case (5.69 → 4.64 eV). Differing from formaldehyde, the GMCPT did not improve the shift. The shifts by GMCPT using the ESP by the present method (GMCPT//SA-MCSCF/1D- and 3D-RISM) were -0.24 and -0.45 eV for 1D- and 3D-RISM-SCF cases, respectively. Those by GMCPT//SS-MCSCF/1D- and 3D-RISM) were -0.36 and -0.36 eV, respectively.

5. Summary

In the present Letter, we have implemented the SA-MCSCF method to the 1D- and 3D-RISM-SCF (as well as MOZ-SCF) schemes. The method was formulated as a quasi-variational problem. The SA-MCSCF equations were derived from the variational condition of the state-average Helmholtz energy with respect to the one- and many-electron wavefunctions variations, while the RISM and closure equations were derived from the variational condition of the state-specific Helmholtz energy with respect to the total and direct correlation function variations.

We have applied the present method to the PECs of NaCl in aqueous solution, the solvent shifts of the n - π^* transition of formaldehyde and π - π^* transition of PNA. The present method (SA-MCSCF/1D-RISM) provided PECs close to those of the state-specific calculation (SS-MCSCF/1D-RISM). The maximum difference was about 0.2 eV. The solvent shifts by the present method (SA-MCSCF/1D- and 3D-RISM) were in good agreement with the experiments, especially in the 3D-RISM-SCF case. In this case, the shift for formaldehyde was 0.24 eV compared with the experimental value of 0.21 eV, while the shift for PNA was -0.96 eV compared with the experimental value of -0.98 eV. In addition, the RDFs of formaldehyde calculated by the present method and SS-MCSCF/1D-RISM were very similar. These results suggest that the state-averaged MCSCF method combined with the 1D- and 3D-RISM-SCF schemes is expected to be an effective tool for chemical properties and reactions in the solution phase along with the pure-state (state-specific) MCSCF method.

Declaration of Competing Interest

None.

Acknowledgments

This work was supported by JSPS Kakenhi [Grant Number:

18K05036 to HN, 16H00842 and 16K05519 to NY]. NY also acknowledges support from the Toyota RIKEN Scholar Program at the Toyota Physical and Chemical Research Institute.

References

- [1] M.W. Schmidt, M.S. Gordon, The construction and interpretation of mcscf wavefunctions, *Annu. Rev. Phys. Chem.* 49 (1998) 233–266.
- [2] K. Ruedenberg, K.R. Sundberg, MCSCF Studies of Chemical Reactions: Natural Reaction Orbitals and Localized Reaction Orbitals, in: J.-L. Calais, O. Goscinski, J. Linderberg, Y. Öhrn (Eds.), *Quantum Sci.*, Plenum, New York, 1976, pp. 505–511.
- [3] B.O. Roos, P.R. Taylor, P.E.M. Siegbahn, A complete active space SCF method (CASSCF) using a density matrix formulated super-CI approach, *Chem. Phys.* 48 (1980) 157–173.
- [4] H. Nakano, K. Hirao, A quasi-complete active space self-consistent field method, *Chem. Phys. Lett.* 317 (2000) 90–96.
- [5] J. Olsen, B.O. Roos, P. Jørgensen, H.J.A. Jensen, Determinant based configuration interaction algorithms for complete and restricted configuration interaction spaces, *J. Chem. Phys.* 89 (1988) 2185–2192.
- [6] J. Ivancić, Direct configuration interaction and multiconfigurational self-consistent-field method for multiple active spaces with variable occupations. II. Application to oxoMn(salen) and N₂O₄, *J. Chem. Phys.* 119 (2003) 9377–9385.
- [7] T. Fleig, J. Olsen, C.M. Marian, The generalized active space concept for the relativistic treatment of electron correlation. I. Kramers-restricted two-component configuration interaction, *J. Chem. Phys.* 114 (2001) 4775–4790.
- [8] S. Ten-no, F. Hirata, S. Kato, A hybrid approach for the solvent effect on the electronic structure of a solute based on the RISM and Hartree-Fock equations, *Chem. Phys. Lett.* 214 (1993) 391–396.
- [9] S. Ten-no, F. Hirata, S. Kato, Reference interaction site model self-consistent field study for solvation effect on carbonyl compounds in aqueous solution, *J. Chem. Phys.* 100 (1994) 7443–7453.
- [10] A. Kovalenko, F. Hirata, Self-consistent description of a metal–water interface by the Kohn-Sham density functional theory and the three-dimensional reference interaction site model, *J. Chem. Phys.* 110 (1999) 10095–10112.
- [11] S. Gusarov, T. Ziegler, A. Kovalenko, Self-Consistent combination of the three-dimensional RISM theory of molecular solvation with analytical gradients and the amsterdam density functional package, *J. Phys. Chem. A* 110 (2006) 6083–6090.
- [12] D. Casanova, S. Gusarov, A. Kovalenko, T. Ziegler, Evaluation of the SCF combination of KS-DFT and 3D-RISM-KH; solvation effect on conformational equilibria, tautomerization energies, and activation barriers, *J. Chem. Theory Comput.* 3 (2007) 458–476.
- [13] H. Sato, A. Kovalenko, F. Hirata, Self-consistent field, ab initio molecular orbital and three-dimensional reference interaction site model study for solvation effect on carbon monoxide in aqueous solution, *J. Chem. Phys.* 112 (2000) 9463–9468.
- [14] N. Yoshida, S. Kato, Molecular Ornstein-Zernike approach to the solvent effects on solute electronic structures in solution, *J. Chem. Phys.* 113 (2000) 4974–4984.
- [15] H. Sato, F. Hirata, S. Kato, Analytical energy gradient for the reference interaction site model multiconfigurational self-consistent-field method: application to 1,2-difluoroethylene in aqueous solution, *J. Chem. Phys.* 105 (1996) 1546–1551.
- [16] T. Mori, S. Kato, Analytical RISM-MP2 free energy gradient method: application to the Schlenk equilibrium of Grignard reagent, *Chem. Phys. Lett.* 437 (2007) 159–163.
- [17] D. Yokogawa, Coupled cluster theory combined with reference interaction site model self-consistent field explicitly including spatial electron density distribution, *J. Chem. Theory Comput.* 14 (2018) 2661–2666.
- [18] R.Y. Shimizu, T. Yanai, Y. Kurashige, D. Yokogawa, Electronically excited solute described by RISM approach coupled with multireference perturbation theory: vertical excitation energies of bioimaging probes, *J. Chem. Theory Comput.* 14 (2018) 5673–5679.
- [19] H. Sato, A modern solvation theory: quantum chemistry and statistical chemistry, *Phys. Chem. Chem. Phys.* 15 (2013) 7450–7465.
- [20] N. Yoshida, T. Ishida, F. Hirata, Theoretical study of temperature and solvent

- dependence of the free-energy surface of the intramolecular electron-transfer based on the RISM-SCF theory: application to the 1,3-dinitrobenzene radical anion in acetonitrile and methanol, *J. Phys. Chem. B.* 112 (2008) 433–440.
- [21] T. Mori, K. Nakano, S. Kato, Conical intersections of free energy surfaces in solution: Effect of electron correlation on a protonated Schiff base in methanol solution, *J. Chem. Phys.* 133 (2010) 064107.
- [22] F. Hirata, *Molecular Theory of Solvation*, Kluwer Academic Publishers, Dordrecht, 2004.
- [23] N. Yoshida, F. Hirata, A new method to determine electrostatic potential around a macromolecule in solution from molecular wave functions, *J. Comput. Chem.* 27 (2006) 453–462.
- [24] M.W. Schmidt, K.K. Baldrige, J.A. Boatz, S.T. Elbert, M.S. Gordon, J.H. Jensen, S. Koseki, N. Matsunaga, K.A. Nguyen, S. Su, T.L. Windus, M. Dupuis, J.A. Montgomery, General atomic and molecular electronic structure system, *J. Comput. Chem.* 14 (1993) 1347–1363.
- [25] T.H. Dunning, Gaussian basis sets for use in correlated molecular calculations. I. The atoms boron through neon and hydrogen, *J. Chem. Phys.* 90 (1989) 1007–1023.
- [26] D.E. Woon, T.H. Dunning, Gaussian basis sets for use in correlated molecular calculations. III. The atoms aluminum through argon, *J. Chem. Phys.* 98 (1993) 1358–1371.
- [27] B.P. Prascher, D.E. Woon, K.A. Peterson, T.H. Dunning, A.K. Wilson, Gaussian basis sets for use in correlated molecular calculations. VII. Valence, core-valence, and scalar relativistic basis sets for Li, Be, Na, and Mg, *Theor. Chem. Acc.* 128 (2011) 69–82.
- [28] E. Cancès, B. Mennucci, J. Tomasi, A new integral equation formalism for the polarizable continuum model: theoretical background and applications to isotropic and anisotropic dielectrics, *J. Chem. Phys.* 107 (1997) 3032–3041.
- [29] J.P. Perdew, M. Ernzerhof, K. Burke, Rationale for mixing exact exchange with density functional approximations, *J. Chem. Phys.* 105 (1996) 9982–9985.
- [30] C. Adamo, V. Barone, Toward reliable density functional methods without adjustable parameters: the PBE0 model, *J. Chem. Phys.* 110 (1999) 6158–6170.
- [31] H. Nakano, R. Uchiyama, K. Hirao, Quasi-degenerate perturbation theory with general multiconfiguration self-consistent field reference functions, *J. Comput. Chem.* 23 (2002) 1166–1175.
- [32] R. Ebisuzaki, Y. Watanabe, H. Nakano, Efficient implementation of relativistic and non-relativistic quasidegenerate perturbation theory with general multiconfigurational reference functions, *Chem. Phys. Lett.* 442 (2007) 164–169.
- [33] A. Noy, I. Soteras, F.J. Luque, M. Orozco, The impact of monovalent ion force field model in nucleic acids simulations, *Phys. Chem. Chem. Phys.* 11 (2009) 10596–10607.
- [34] J. Wang, R.M. Wolf, J.W. Caldwell, P.A. Kollman, D.A. Case, Development and testing of a general amber force field, *J. Comput. Chem.* 25 (2004) 1157–1174.
- [35] J. Wang, W. Wang, P.A. Kollman, D.A. Case, Automatic atom type and bond type perception in molecular mechanical calculations, *J. Mol. Graph. Model.* 25 (2006) 247–260.
- [36] H.J.C. Berendsen, J.R. Grigera, T.P. Straatsma, The missing term in effective pair potentials, *J. Phys. Chem.* 91 (1987) 6269–6271.
- [37] Y. Zeiri, G.G. Balint-Kurti, Theory of alkali halide photofragmentation: potential energy curves and transition dipole moments, *J. Mol. Spectrosc.* 99 (1983) 1–24.
- [38] M.B. Robin, *Higher Excited States of Polyatomic Molecules*, Academic Press, New York, 1974.
- [39] T. Bercovici, J. King, R.S. Becker, Formaldehyde: comprehensive spectral investigation as a function of solvent and temperature, *J. Chem. Phys.* 56 (1972) 3956–3963.
- [40] S. Millefiori, G. Favini, A. Millefiori, D. Grasso, Electronic spectra and structure of nitroanilines, *Spectrochim. Acta, Part A* 33 (1977) 21–27.
- [41] C.L. Thomsen, J. Thøgersen, S.R. Keiding, Ultrafast charge-transfer dynamics: studies of *p*-Nitroaniline in water and dioxane, *J. Phys. Chem. A.* 102 (1998) 1062–1067.
- [42] S.A. Kovalenko, R. Schanz, V.M. Farztdinov, H. Hennig, N.P. Ernsting, Femtosecond relaxation of photoexcited para-nitroaniline: solvation, charge transfer, internal conversion and cooling, *Chem. Phys. Lett.* 323 (2000) 312–322.